Available online at www.sciencedirect.com
SCIENCE DIRECT
ELSEVIER
Journal of the European Ceramic Society 26 (2006) 2365–2372
ECERS
www.elsevier.com/locate/jeurceramsoc

Structural and proton conductivity study of P_2O_5-TiO_2-SiO_2 glasses

T. Uma *, S. Izuhara, M. Nogami **

Department of Material science and Engineering, Nagoya Institute of Technology, Showa, Nagoya, 466-8555, Japan

Received 23 January 2005; received in revised form 8 April 2005; accepted 15 April 2005
Available online 27 June 2005

Abstract

Proton conducting membranes for hydrogen fuel cell applications are being developed using sol–gel-derived P_2O_5-TiO_2-SiO_2 glasses. The present work is devoted to the structural analysis of P_2O_5-TiO_2-SiO_2 glasses containing controlled pore sizes and the surface area of the glasses reaching a maximum 410 m^2/g, while the average pore diameter is about 2.4 nm. They were characterized by nitrogen adsorption–desorption measurements, thermal measurement as well as FTIR spectroscopy. The structural studies were based on the evolution of the intensities and profiles of certain characteristics bands in the FTIR spectra. In order to increase proton conductivity at low relative humidity, the result suggests that the mobility of proton in the P_2O_5-TiO_2-SiO_2 glasses increases with decreasing O–H bonding strength. An H_2/O_2 fuel cell was constructed using the P_2O_5-TiO_2-SiO_2 glasses as electrolyte and Pt/C-loaded carbon paper sheets as electrodes. Results show that the performance of the cell is an output power of 88 $\mu W/cm^2$ at 30 °C with humidity.

Keywords: Fuel cell; Glass; FTIR; TiO_2; Proton conductivity

1. Introduction

Proton (H^+) transport in solids has attracted much attention because of its potential use in clean energy fields, such as fuel cells, batteries and chemical sensors. An entire class of materials has gained increasing interest as proton conductors: polymers, oxide ceramics, intercalation compounds etc. A brief overview of the past and present state of solid state protonic conductors has been reported.[1,2] The classification of proton conductors according to the preparation method, chemical composition, structural dimensionality, mechanism of conduction etc., have been summarized in a comprehensive book on proton conductors.[3]

Although these materials can be prepared by a conventional ceramic route, sol–gel synthetic methods are a viable alternative not only because they represent a lower cast technology but also because better mixing of the starting materials can be achieved on the molecular scale. A number of fast-protonic conductors, organic or inorganic crystalline and amorphous have been prepared during the past two decades,[4] which are categorized into two types based on their operating temperatures. They are the hydrated crystalline compounds,[5] and perflurinated ionomers[6] and both showing high conductivities of $\sim 10^{-2}$ S/cm below 100 °C, but their chemical degradation limits the use in practical applications. Many classes of protonic conductors are represented by members which at some temperature exhibit protonic conductivities of up to 10^{-3} to 10^{-2} S/cm. This typically represents a maximum as a function of temperature: at higher temperatures, the protonic conduction decreases because of reversible or irreversible loss of vehicle water (e.g., polymer), because of decomposition or melting of hydrates and hydroxides or acid salts or because of reversible loss of protons (water) from oxides. Thus, proton conductors are generally functional over relatively narrow temperature ranges. On the other hand, fast-proton conducting glasses, if developed, extend beyond the limitation of the above compounds, because of their high chemical and mechanical stability and easy formation into films and plates. Sol–gel-derived alkaline phosphate glasses have been developed as fast-proton conducting

* Corresponding author. Tel.: +81 52 7355285; fax: +81 52 7355285.
** Corresponding author.
E-mail address: nogami@mse.nitech.ac.jp (T. Uma).

0955-2219/$ – see front matter © 2005 Elsevier Ltd. All rights reserved.
doi:10.1016/j.jeurceramsoc.2005.04.013

materials due to their large capacity for hydroxyl groups. Despite the increased proton conductivity, the alkaline phosphate glasses derived from sol–gel process have a limited phosphate concentration due to the decrease in mechanical strength and chemical stability with increasing phosphorous concentration.[7,8]

We have successfully prepared P_2O_5-SiO_2 binary glasses using a sol–gel technique and exhibiting high conductivities of $\sim 10^{-2}$ S/cm at room temperature.[9–11] It was reported that the chemical stability of glasses are related to the termination of P^{5+} ions with Ti–OH bonds.[12] The aim of the present work is to improve the high proton conductivity of P_2O_5-TiO_2-SiO_2 glasses for possibility of increasing a H_2/O_2 cell performance with suitable electrode/electrolyte working condition. The chemical stability of the glasses is important factor if these materials are to be appreciated for practical application of the fuel cell electrolytes.

2. Experimental procedure

2.1. Sample preparation

The glasses were prepared by the sol–gel technique. Appropriate quantities of Ti $(OC_4H_9)_4$ and Si $(OC_2H_5)_4$ and PO $(OCH_3)_3$ were partially hydrolyzed with a solution of H_2O (as 0.15 N HCl) and C_2H_5OH in mole ratios of 1:1 per mole of Si $(OC_2H_5)_4$. The mixture was stirred for 30 min and their Ti $(OC_4H_9)_4$ (99%, Kishida Chemical) mixed with C_2H_5OH in mole ratio of 1:10 was added under continuous stirring for 1 h. PO $(OCH_3)_3$ (98%, Nacalai Tesque) dissolved in C_2H_5OH with five times moles of H_2O was added to solution drop-by-drop under stirring. The phosphorus compound was mixed with the total solution and was stirred for about 1 h. $HCONH_2$ (1–3 ml) was added for 5 g oxide glass in standard solution followed by 30 min stirring. Finally, a clear solution was obtained and it was kept carefully for 1 month, which led to the formation of a stiff (0.5–1.5 mm thickness) gel plates. This led to the complete hydrolysis of the alkoxide. The gels were dried at room temperature and followed by heat treatment about 50–600 °C for 2 h (Fig. 1).

2.2. Characterization

X-ray diffraction (XRD) patterns were recorded form the samples by a Bruker AXS D-5005 diffractometer using Cu Kα radiation in steps size of 0.02° and count time of 1.2 s per point (20 between 5 and 55°). FTIR measurements were made in the range 400–4000 cm^{-1} using a JASCO FTIR-460 spectrometer. Thermogravimetric (TG) and differential thermal analysis (DTA) were performed with SSC-5200 (SEIKO Instrument) from room temperature to 800 °C with heating rate of 5 °C/min using powder samples. The pore properties were studied by a nitrogen gas adsorption–desorption analyzer (NOVA-1000, Quantochrome) and also the specific surface area calculated using BET method. Electrical conductivity measurements were performed in the frequency range 0.1 Hz to 1 MHz with signal amplitude of 10 mV using a Solatron 1260 impedance/grain phase analyzer in a simple two-electrode system. Experiments were carried out at 30–90 °C under a relatively humid atmosphere. The temperature was raised stepwise and the measurements were carried out after keeping at each temperature for 2 h. During the conductivity measurement the samples were kept in a constant humidity chamber. The temperature and humidity of the chamber were controlled at 30–90 °C and 40–90% RH, respectively. Gel-derived TiO_2-SiO_2 particles prepared by sol–gel route and a brief explanation of structural and pore properties studies were reported.[13] In a previous work[11], we have shown that the P_2O_5-SiO_2 binary glasses also exhibiting high conductivities of $\sim 10^{-2}$ S cm^{-1} at room temperature. Further, we optimized the most of the system for improve the high proton conductivity in order to select this compositions studied for our present work. The chemical stability of these glasses increased significantly on the addition of TiO_2.

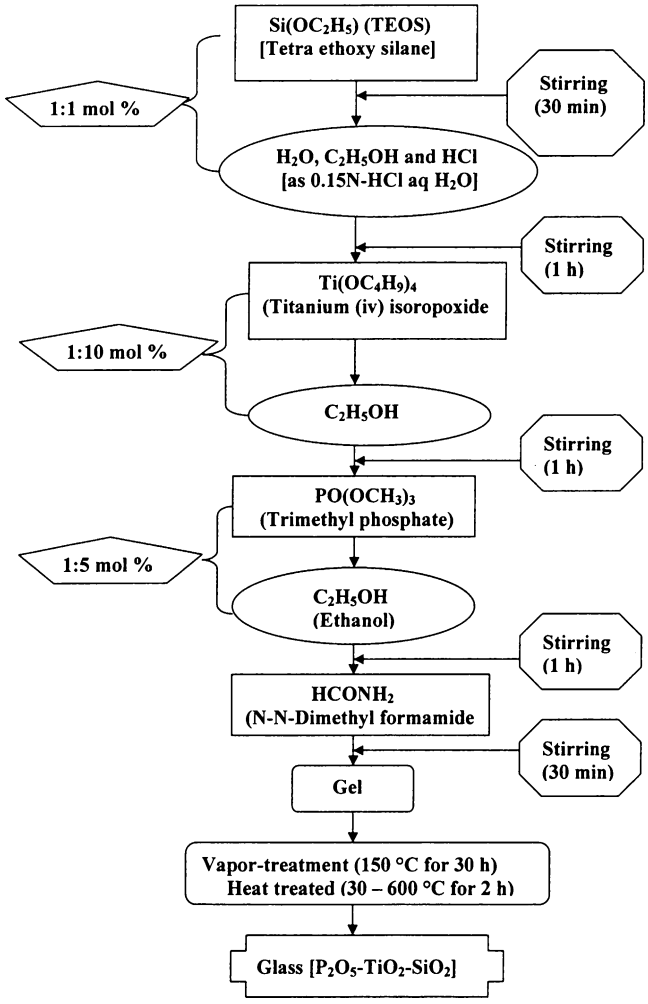

Fig. 1. Flow chart of the sol–gel synthesis of P_2O_5-TiO_2-SiO_2 glasses.

The H_2/O_2 fuel cell tests were carried out for the electrolyte/electrode assemblies which consisted of the glass

membrane as an electrolyte with Pt/C-loaded (0.2 mg/cm^2) carbon paper sheets as electrodes. The catalyst ink [mixing Pt/C powder (0.2 mg/cm^2), Nafion solution (5 wt.%), Polytetraflouroethlene (PTFE) (10 wt.%) and solvent (mixture of water and ethanol)] was painted onto wet-proofed carbon paper sheet. These electrodes were dried at 150 °C for 1 day to remove water and ethanol. The thickness of the catalyst layer is dependent on the loading of platinum supported carbon. These type electrodes were used for the fuel cell test. We have been making membrane electrode assemblies with glasses as an electrolyte and electrode on Pt/C-loaded were used for electrochemical measurements. Current–voltage profiles in the fuel cells were performed under humidity condition by using an electrochemical measurement system (SI 1287-Solatron). Temperature of the cell was controlled by NF (Japan product) and flow rates of hydrogen for anode and oxygen for cathode were 100–100 mL/min at constant atmospheric pressure (Fig. 2).

3. Results and discussion

3.1. Structural studies

XRD of the glass heat-treated at 600 °C, do not exhibit any sharp peaks which is indicative of non-crystalline nature of the materials. FTIR spectroscopy is a powerful tool to study the structural changes in P_2O_5-TiO_2-SiO_2 glasses (Fig. 3). The low wave number region of the FTIR absorption spectrum has been used extensively to characterize TiO_2-SiO_2 mixed oxides. According to the data, absorption bands are seen with the titania-silica mixed oxides, suggesting that the absorption may be associated with the presence of the Ti–O–Si bonds. The band at 971 cm^{-1} is assigned to a Si–O–Ti stretching. This band has been ascribed to a vibration involving SiO_4 tetrahedra bonded to a fourfold coordinated titanium atom indicates a good mixing of Ti and Si at

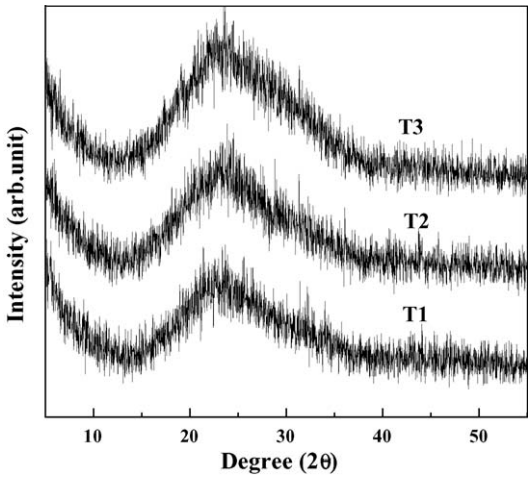

Fig. 2. X-ray diffraction patterns of P_2O_5-TiO_2-SiO_2 glasses prepared by sol–gel method.

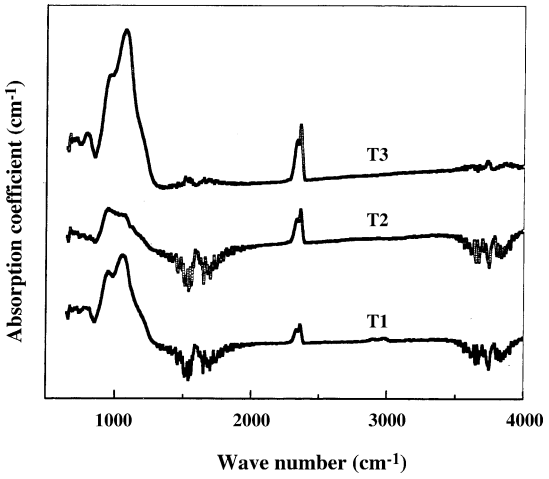

Fig. 3. FTIR plots of P_2O_5-TiO_2-SiO_2 glasses prepared by sol–gel method.

atomic level.[14] The strong absorption in the frequency region of 700–800 cm^{-1} corresponds to Ti–O–Ti bonding and indicates the formation of a titanium oxide network.[15] The intensity of the absorption can be represented to Si–O–Si stretching modes at around 800–1300 cm^{-1} and the intercity varies with the amount of P_2O_5 content in the sample. The 1530, 1650 and 2350 cm^{-1} bands were assigned to the hydroxyl-related vibrational modes. Such conclusion follows from (i) a similarity in the location of these bands and the known hydroxyl-related bands in the spectra of various hydrate crystals,[16–18] (ii) substantial variations in the peak absorptivities and oscillator strengths of these bands depending on the water content and temperature of glass melting, and (iii) a strict correlation between variations in the peak absorptitives of these bands and the known hydroxyl-related 2350 cm^{-1} band. In addition, the peaks common for all silicate structures at below around 1000 cm^{-1}, due to one of the stretching and bending vibrations of Si–O or SiOH were observed.[19] Here, it was considered that the peak near 940 cm^{-1} is associated with the Si–O stretching in Si–O–Ti^{4+} sequence involving tetrahedrally coordinated Ti^{4+} ions, or $(SiO)_3$-OH due to the hydroxylated surface or non-bridged groups in network. This may be due to the condensation of structural hydroxyl groups at higher heat-treatment of 600 °C. This fact is also evident from the FTIR spectra. It is seen that the intensity of the peaks at ∼3700 and 1600 cm^{-1} representative of the –OH group and external water molecules respectively diminishes at higher temperature. Due to this reason, the high conductivity is obtained at high temperature.

3.2. Thermal studies

TG/DTA studies were made to identify thermal stability of the P_2O_5-TiO_2-SiO_2 glass samples. From the TGA curves, it is found that all samples show thermal dehydration. Thermograms indicate 5.5 and 7.2% weight loss within the temperature range of 30–400 °C corresponding to the loss of water molecules, after which a gradual weight loss

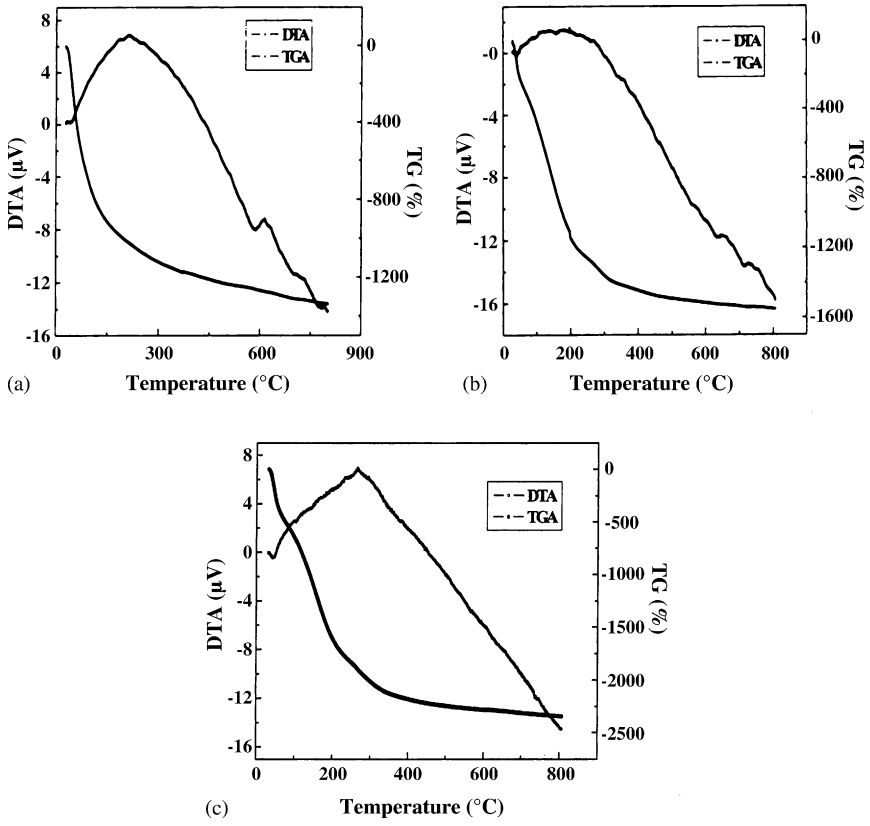

Fig. 4. TG-DTA curve for the P_2O_5-TiO_2-SiO_2 glasses: (a) $5P_2O_5$-$6TiO_2$-$89SiO_2$ (mol%), (b) $7P_2O_5$-$6TiO_2$-$85SiO_2$ (mol%) and (c) $9P_2O_5$-$6TiO_2$-$85SiO_2$ (mol%).

is observed till ∼500 °C (Fig. 3(a)). This may be due to the condensation of structural hydroxyl groups. Beyond ∼100 °C and up to around ∼400 °C, a broad exothermic peaks associated with a weight loss is observed. There is no endothermic peak up to 500 °C, which indicates that there is no phase change. One sharp endothermic peak is also observed around at 600 °C. The condensation reaction in this region proceeds with increasing temperature, resulting obtained in the formation of strengthened glass structure. Fig. 3(b) shows that the weight decreases gradually above around ∼310 °C is observed in the TG curve. Above 600 °C the sharp endothermic peak was disappeared. The gradual weight loss of 9.6 and 12.2% within 35–350 °C temperature range is associated with the condensation of OH groups in glass network structure. In Fig. 3(c), an exothermic peak at ∼285 °C is observed and in addition another endothermic is also observed at ∼44 °C in DTA curve which may be attributed in moisture. In the TGA curve, the weight decreases gradually at around ∼300 °C and weight loss of 7.8 and 10% calculated within same temperature. This agrees with the DTA results. These results indicate that the sample is stable up to about ∼300 °C (Fig. 4).

3.3. Pore studies

The textural properties of the glass determined from the nitrogen adsorption and desorption isotherms are shown in Table 1. The adsorption–desorption isotherms and pore size distribution of a P_2O_5-TiO_2-SiO_2 glasses (T1–T3) calcined at 250 °C are shown in Fig. 5(a)–(c). The BJH desorption pore size distribution is shown in Fig. 5 (d)–(f). It shows that by increasing the amount of P_2O_5 in the mixture a decrease in the BET area occurred, while mean pore diameter increased moderately (Table 1). The decrease in surface area may be due to an increase in the phosphorous domains in the interconnected silica structure. In the compositions, the hydroxyl groups in phosphate glasses are strongly hydrogen bonded with the counter oxygen atoms. Pores obtained on the glass

Table 1
Pore properties of P_2O_5-TiO_2-SiO_2 glasses heat-treated at 600 °C

sample	P_2O_5-TiO_2-SiO_2 glasses (mol%)	Average pore size (nm)	Average pore volume (cm^3/g)	Specific surface area (m^2/g)
T1	5-6-89	2.35	0.24	402 ± 2
T2	7-6-87	2.42	0.22	369 ± 2
T3	9-6-85	2.60	0.13	203 ± 2

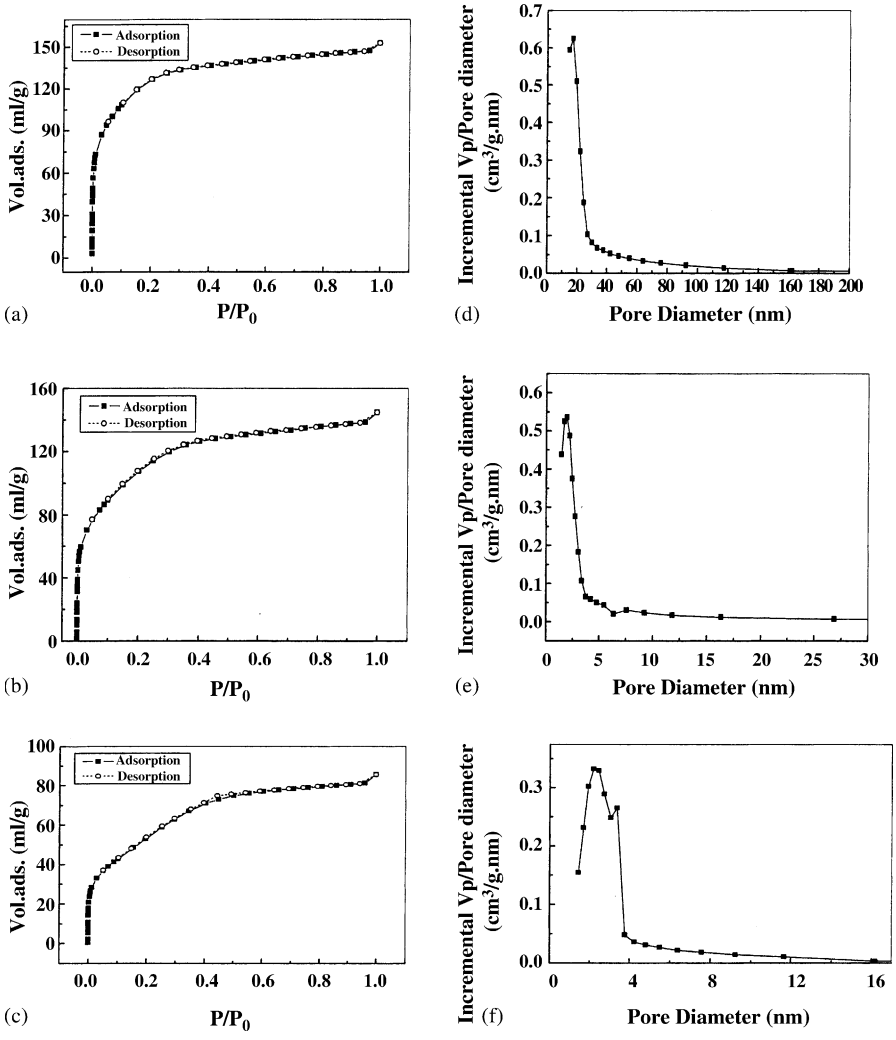

Fig. 5. N_2 adsorption isotherms (a)–(c) and BJH pore-size distributions (d)–(f) for P_2O_5-TiO_2-SiO_2 glasses (T1–T3) heat-treated at 600 °C.

surface are fulfilled with rich part of POH group. The proton in the POH group is strongly hydrogen-bonded with the water molecules compared with that of the SiOH groups in silica network of the core structure. The pore properties of the glasses play an important role on the proton conduction in glasses. The water molecules are bonded with the hydroxyl groups, such as POH, TiOH, and SiOH bonds. The porosity and average pore size of the P_2O_5-TiO_2-SiO_2 glasses appear to be the main factors, which are influence of the proton conductivity. The proton conductivity increases with increasing number of adsorbed water molecules. So the pore properties are one of the important factors to determine the proton conduction in glasses. The absence of hysteresis loop in the desorption branch in Fig. 5(d)–(f) indicates that the pores are smooth and cylindrical.

3.4. Conductivity studies

The AC conductivity σ was determined by cole–cole plots using an impedance analyzer (Solartron SI 1260) in the frequency range 0.1 Hz to 1 MHz. These measurements were carried out the temperature range 30–90 °C with relative humidity 40–90% (Figs. 6 and 7). The temperature dependence of conductivity ($\log \sigma$ versus $1/T$) for the P_2O_5-TiO_2-SiO_2 glasses for optimized compositions is shown in Fig. 6. The temperature increases the conductivity values are also found to increase (Table 2) for all samples. The proton dissociated from the POH bonds become more mobile which increases the conductivity and the protons transfer is through the water molecules in the pores by hopping mechanism.[20,21] The conductivity of sample T2 ($7P_2O_5$-$6TiO_2$-$85SiO_2$ mol%) increases with increasing temperature from 30 to 90 °C and the value has the maximum of 1.5×10^{-2} S/cm at 90 °C. Fig. 7 shows that the relative humidity dependence of conductivity for the P_2O_5-TiO_2-SiO_2 glasses at 30 °C. The conductivity values for P_2O_5-TiO_2-SiO_2 glasses are found to be in the range 10^{-4} to 10^{-2} S/cm at RH% (Table 3). The effect of P_2O_5, increasing proton conduction in the glass media, because of strong hydrogen bonding characteristics of the POH bond compared

Table 2
Conductivity values of P_2O_5-TiO_2-SiO_2 glasses at different temperatures

Sample number	σ (S/cm) values						
	30 °C	40 °C	50 °C	60 °C	70 °C	80 °C	90 °C
Tl	1.59×10^{-3}	1.81×10^{-3}	2.01×10^{-3}	2.44×10^{-3}	2.61×10^{-3}	2.84×10^{-3}	2.91×10^{-3}
T2	8.70×10^{-3}	1.01×10^{-2}	1.11×10^{-2}	1.21×10^{-2}	1.31×10^{-2}	1.41×10^{-2}	1.47×10^{-2}
T3	3.35×10^{-3}	4.39×10^{-3}	5.83×10^{-3}	6.70×10^{-3}	6.93×10^{-3}	7.32×10^{-3}	7.62×10^{-3}

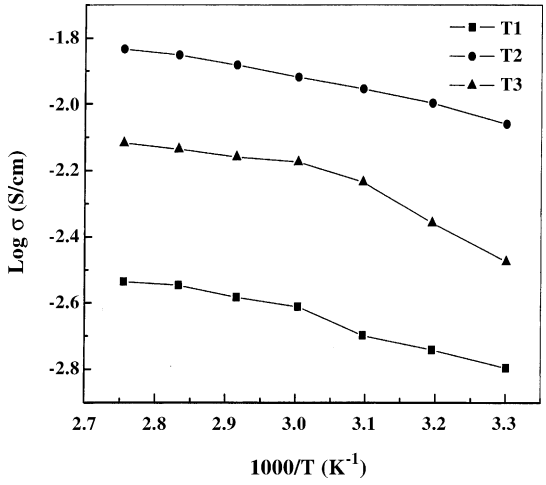

Fig. 6. Arrhenius plot of log conductivity against reciprocal temperature for P_2O_5-TiO_2-SiO_2 glasses heat-treated at 600 °C: (Tl) $5P_2O_5$-$6TiO_2$-$89SiO_2$ (mol%), (T2) $7P_2O_5$-$6TiO_2$-$87SiO_2$ (mol%) and (T3) $9P_2O_5$-$6TiO_2$-$85SiO_2$ (mol%).

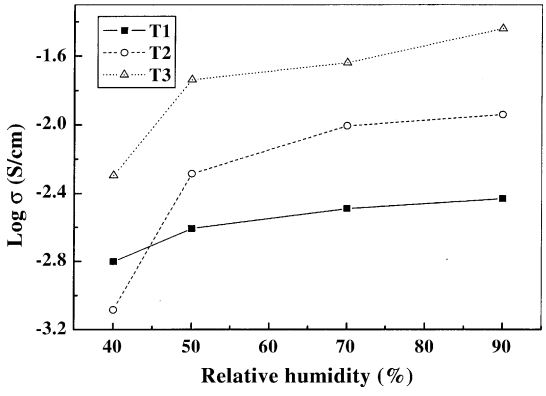

Fig. 7. Arrhenius plot of the conductivity P_2O_5-TiO_2-SiO_2 glasses with different (40–80%) humidity conditions at 30 °C: (T1) $5P_2O_5$-$6TiO_2$-$89SiO_2$ (mol%), (T2) $7P_2O_5$-$6TiO_2$-$87SiO_2$ (mol%) and (T3) $9P_2O_5$-$6TiO_2$-$85SiO_2$ (mol%).

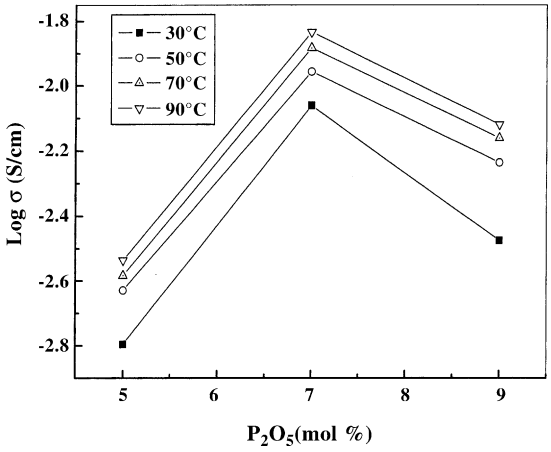

Fig. 8. Composition in P_2O_5 dependence of conductivity for P_2O_5-TiO_2-SiO_2 glasses at 30–90 °C temperature with 70% relative humidity.

with SiOH bond. The conductivity of the glass increases with an increase in the relative humidity and shows a maximum value 3.6×10^{-2} S/cm at 90% humidity for the sample T3. This suggests the mechanism of transportation as Grotthus type[22] where the conductivity depends on the ability of the water located on the surface to rotate and participate. In comparison, the conductivity is nearly an order of magnitude higher in humid atmosphere. The increase in conductivity is clearly due to water uptake by the glass sample. However, we observed a high conductivity of 6.89×10^{-2} S/cm at room temperature with dry condition. Further, the overall conductivity values indicate that the chemical stability of P_2O_5-TiO_2-SiO_2 glass is a suitable electrolyte for fuel cells operating at the low temperature. Fig. 8 shows the concentration of P_2O_5 relative with conductivity at 30–90 °C temperature dependence with relative humidity of 70% for all compositions. It is observed that the conductivity decreases with increasing P_2O_5 ratio above 7 mol% in the composition. It indicates that there are two competing effects at play in glass media. At low concentration of P_2O_5 loadings, the conductivity increases; it may be due to the increase in the

Table 3
Conductivity values of P_2O_5-TiO_2-SiO_2 glasses in humidity atmosphere (40–90%) at 30 °C

Sample number	P_2O_5-TiO_2-SiO_2 glasses (mol%)	σ (S/cm) values			
		40%	50%	70%	90%
T1	5-6-89	1.58×10^{-3}	2.47×10^{-3}	3.23×10^{-3}	3.71×10^{-3}
T2	7-6-85	8.26×10^{-4}	5.19×10^{-3}	9.86×10^{-3}	1.14×10^{-2}
T3	9-6-85	5.07×10^{-3}	1.82×10^{-2}	2.29×10^{-2}	3.62×10^{-2}

conductive layers. At higher P_2O_5 concentrations, phase discontinuities and dilution effects will predominate instead and result in low conductivities (Table 2). It may be the nature of the conduction mechanism can vary from hopping in a disordered random network potential to a percolation pathway involving higher mobilities in a particular region of homogeneous glasses, with slower motions in the intervening structure.[23–26] These results strongly suggest that the conductivities are enhanced by the incorporation of P_2O_5 content in glass, despite the difference in their pore surfaces.

The proton conduction is strongly affected by the nature of the textural properties. We found that the highest proton conductivity of $9P_2O_5$-$6TiO_2$-$85SiO_2$ glass is 3.6×10^{-2} S/cm at 90% humidity (sample T3). Generally, such glasses with large pore volume and large surface area possess the capability to absorb a large amount of water in the pores. The surface area and pore size correspond to the concentration of the surface OH groups and the adsorbed water molecules, respectively. The water content increases with the increasing humidity and all the pores are filled with water molecules. It was found that the dependence of water adsorption on the humidity is analogues to the N_2-gas adsorption isotherm. Further adsorption of water molecules leads to the multilayer of water molecules, which are physically bound in pores; it is necessary for glasses to be exposed in high humidity for high conductivity. We noted that the high proton conductivity for sample T3 (Table 3) with large pore size such glass containing appropriate amount of P_2O_5 (9 mol%), and interesting to observed the average pore size and pore volume is 2.6 nm and 0.13 cm^2/g for that sample T3. The pore properties indicate the OH groups on the hydrogel network would condense and form Si–O–Si bridges during heat treatment or gel drying condition. The pore volume and surface area both decreases continually depends heat treatment and nature of glass preparation, the shape of the pore size distribution remains basically the same. For this reason, heating caused the dehydration–condensation reaction between the hydroxyl bonds. During this reaction, the gels shrunk and resulting in the reduction of surface and pore volume. The porous SiO_2 structure remains unchanged in glass heated at 600 °C, the surfaces of which are terminated with the hydroxyl bonds.

3.5. Fuel cell studies

In the present work, we observed that the cell voltage (0.7–0.9 V), current density (50–217 μA/cm^2) and power density (20–88 μW/cm^2) throughout the fuel cell performance. Fig. 9, the open circuit voltage rise-up smoothly increases the operating time. It seems the performance stability of the fuel cell is constant during operating time. But this condition is not always same to maintain, reason for that the contact between electrolyte/electrode. Fig. 10(a) and (b), shows that the cell voltage versus current density and power density plots for a fuel cell using electrolyte/electrode assemblies which consist of $9P_2O_5$-$6TiO_2$-$85SiO_2$ (Sample T3) glass as an electrolyte and Pt/C-loaded carbon paper sheets

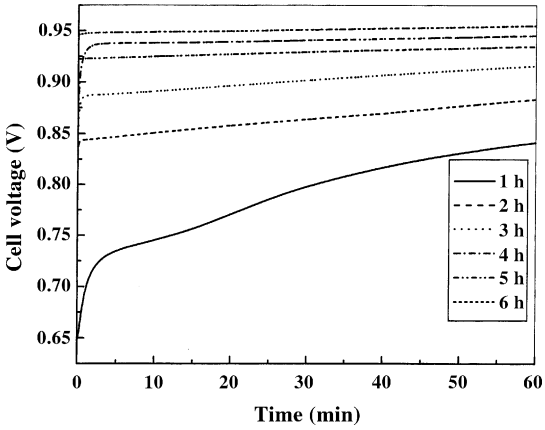

Fig. 9. Variation in cell voltage for operation time at 30 °C under relative humidity with constant atmosphere.

as electrodes. The cell operated under constant atmospheric pressure and the gas flow rate to anode and cathode side was 100 mL/min at 30 °C with relative humidity condition. Generally, the electrochemistry reaction, which takes place inside a fuel cell, hydrogen (H_2) flows over the anode (the negative electrode) and splits into positively charged hydrogen ions, and electrons which carry a negative charge. The electrons flow through the anode to the external circuit, performing useful work (this is the electrical current generated) while the hydrogen ions pass through the anode and into the electrolyte, moving towards the cathode (the positive electrode). The electrons eventually return to the cathode, which is sup-

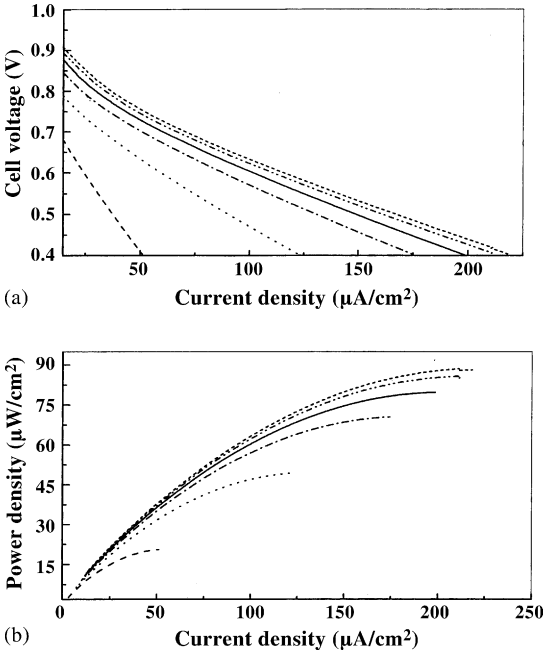

Fig. 10. Cell voltage vs. current density (a) and power density vs. current density (b) for a for operation time at 35 °C under relative humidity with fuel cell using an electrode/electrolyte (Pt/C catalyst = 0.2 mg/cm^2) consisting of the $9P_2O_5$-$6TiO_2$-$85SiO_2$ glasses. The cell operated at 30 °C under humidity atmosphere.

plied with oxygen (O_2). At this point the electrons, hydrogen ions and oxygen react to form water (H_2O). The cell assemble is clamped between two gas flow field compartments to produce a single cell. When hydrogen is fed to the anode compartment, and oxygen to the cathode compartment, an electrical potential of approximately 1 V builds up. When anode and cathode are externally connected by an electrical load, a current is produced and hydrogen and oxygen are consumed. The power increases as a function of load indicating an almost parabolic curve. The operating time increases in the cell significantly improve the cell voltage at low current densities. This performance of the cell is still low for the practical application. However, these results demonstrate that the fuel cell using the glass material as an electrolyte can continuously operate at low temperature with low humidity. Moreover, the electrolyte had a steady performance over time, without showing any signs of chemical or mechanical degradation.

4. Conclusions

The P_2O_5 concentration influences the properties of glass and their structures and thermal stability also understood based on FTIR, Nitrogen adsorption–desorption, TG/DTA and conductivity measurements. The proton conductivity of the P_2O_5-TiO_2-SiO_2 glass increases with an increasing temperature in relative humidity and shows a maximum value of 3.6×10^{-2} S/cm at 90% corresponding to the sample T3 ($9P_2O_5$-$6TiO_2$-$85SiO_2$ mol%). The weight loss in TGA curves are assigned to the physically adsorption of water to the P_2O_5-TiO_2-SiO_2 glass in the step before dehydration. The value of power density of the fuel cell (20–88 $\mu W/cm^2$) increased with an increase in operating time in the relative humidity and atmosphere pressure condition. Based on the above results, the internal contact between electrode and electrolyte is not satisfied and overall cell resistance is high. In order to reduce the interfacial resistance, it is possible to infer that a power density will be increased. Further, we should be optimize the performance of the electrode/electrolyte assemble working condition for electrochemical measurements and improve the power density based on current–voltage characteristics.

Acknowledgement

The authors are grateful to COE program in Nagoya Institute of Technology, Japan for financial support.

References

1. Alberti, G. and Casciolo, M., *Solid State Ionics*, 2001, **145**, 3.
2. Norby, T., *Solid State Ionics*, 1999, **125**, 1.
3. Ikawa, H., In *Proton conductors*, ed. P. h. Colamban. University Press, Cambridge, 1992, p. 190.
4. Colomban, P., Proton conductors, *Chem. Sol. State Mater*. **2**; Cambridge, London, 1992.
5. Kobets, L. V., Kolevich, T. A. and Umreiko, D. S., *Koord. Khim.*, 1978, **4**, 1856.
6. Verbrugge, M. K. and Hill, R. F., *J. Electrochem. Soc.*, 1990, **137**, 3770.
7. Abe, Y., Li, G., Nogami, M. and Kasuga, T., *J. Electrochem. Soc.*, 1996, **143**(1), 144.
8. Nogami, M. L., Nagao, R., Makita, K. and Abe, Y., *Phys. Lett.*, 1997, **71**(10), 1.
9. Nogami, M., Matsushita, H., Kasuga, T. and Hayakawa, T., *Electrochem. Solid-State Lett.*, 1999, **2**, 415.
10. Nogami, M., Matsushita, H., Goto, Y. and Kasuga, T., *Adv. Mater.*, 2000, **12**, 1370.
11. Nogami, Goto, Y., Tsurita, Y. and Kasuga, T., *J. Am. Chem. Soc.*, 2001, **84**, 2553.
12. Nogami, M., Suwa, M. and Kasuga, T., *Solid State Ionics*, 2004, **166**, 39.
13. Yu, H. F. and Wang, S. M., *J. Non-Cryst. Solids*, 2000, **261**, 260.
14. Beghi, M., Chiurlo, P., Costa, L., Palladino, M. and Pirini, M. F., *J. Non-Cryst. Solids*, 1992, **145**, 175.
15. Burgos, M. and Langlet, M., *Thin Solid Films*, 1999, **349**, 19.
16. Miller, F. and Wilkins, C., *Anal. Chem.*, 1952, **24**, 1253.
17. Braunholtz, J. T., Hall, G. E., Mann, F. G. and Sheppard, N., *J. Chem. Soc.*, 1959, **29**, 868.
18. Ryskin, Y. I. and Stsvitskaya, G. P., *Opt. Spektrosk (in Russian)*, 1960, **8**, 606.
19. Liu, Z. and Davis, R. J., *J. Phys. Chem.*, 1994, **98**, 1253.
20. Nogami, M. and Abe, Y., *Phys. Rev. B*, 1997, **18**, 12108.
21. Nogami, M., Nagao, A. and Wong, C., *J. Phys. Chem., B*, 1998, **102**, 5772.
22. Clearfield, A., *J. Mol. Catal.*, 1988, **88**, 125.
23. Pechenik, A., Susman, S., Whitmore, D. H. and Ratner, M. A., *Solid State Ionics*, 1986, **18/19**, 403.
24. Ratner, M. A. and Schriver, D. F., *Chem. Rev.*, 1988, **88**, 109.
25. Ratner, M. A. and Nitzan, A., *Solid State Ionics*, 1988, **28**, 3.
26. Malugani, J. P., Tachez, M., Mercier, R., Dianoux, A. J. and Chieux, P., *Solid State Ionics*, 1987, **23**, 189.